Fiber Optic Sensor for High-Sensitivity Salinity Measurement

Jose Rafael Guzman-Sepulveda, Victor Ivan Ruiz-Perez, Miguel Torres-Cisneros, Jose Javier Sanchez-Mondragon, and Daniel Alberto May-Arrioja

***Abstract*— A highly sensitive salinity sensor based on a two-core optical fiber is demonstrated for both high- and low-concentration regimes. Salinity of several aqueous solutions is measured in the ranges from 0 to 5 mol/L and from 0 to 1 mol/L with sensitivities of 14.0086 and 12.0484 nm/(mol/L), respectively. The achieved sensitivity is ∼19 times higher than that recently reported for polymide-coated photonic crystal fibers.**

***Index Terms*— Fiber optics sensor, in-fiber directional coupler, salinity sensor.**

I. Introduction

SALINITY sensing is essential to climate models and chemical oceanography because it is one of the fundamental parameters of the seawater equation of state [1], but it also plays an important role in chemical and biological analysis for manufacturing processes and protection of ecosystems. Due to the presence of chlorine ions, salinity measurement has been traditionally performed based on the electrical conductivity of water. However, this technique clearly presents serious disadvantages, such as the susceptibility to electromagnetic interference and the fact that other contaminants can alter the electrical conductivity of the sample leading to errors in the measurements [2]. Furthermore, in terms of the efficiency of the salinity-conductivity and the salinity-density datasets, it has been demonstrated that the refractive index (RI) correlates to density 80% better than conductivity since conductivity cannot account for species that may contribute to density but do not measurably conduct electricity [3]. In this regard, a growing interest on fiber optic sensors has arisen due to their well known characteristics of compactness, high sensitivity, *in situ* measurement, and immunity to external electromagnetic interference.

The majority of fiber optic salinity sensors developed to date are based on fiber Bragg gratings (FBG) [4]–[6]. Nevertheless, there are some other proposals based on different principles of operation, such as photonic crystal fibers [7], displacement and differential measurements [8], [9], interferometry [10], and more recently those based on fiber resonators [11], [12], that have demonstrated to be highly effective for salinity sensing. In terms of FBG, special equipment and complex fabrication procedures are often involved when inscribing the grating; and temperature compensation is often achieved by using an additional grating, which implies double-grating fabrication process. In terms of salinity sensors based on differential measurements and resonators, the use of simple sensing elements arises as an outstanding advantage but they often require more complex characterization of the resonator/array response. Furthermore, additional signal processing techniques for ambiguity treatment or intensity compensation are often required for compensation/correction of the experimental measurement. Even if FBG are considered as a viable option, they exhibit low sensitivity, which can be improved, similarly to photonic crystal fibers, by using polymide coatings, but then additional complexity related to the film coating process could impact the cost of the fiber sensor. A similar situation occurs for in-fiber interferometers since they exhibit small interaction lengths and high sensitivity, but they require special equipment to fabricate the cavities in the fiber.

In this letter a simple and compact fiber optic sensor based on a Two-Core fiber (TCF) is demonstrated to perform high-sensitivity salinity measurements. The suitability and high sensitivity of the proposed sensor, which measures the degree of salinity of the water through the RI of the saline solution in which it is immersed, is demonstrated for high- and low-concentration ranges. Salinity measurements in the range from 0 to 5 M (M is mol/L) and in the range from 0 to 1 M were performed with sensitivities of 14.0086 nm/M and 12.0484 nm/M, respectively. The achieved sensitivity is approximately 19 times larger than that recently reported for polymide-coated photonic crystal fibers and polymide-coated FBG [7].

II. Principle of Operation

A picture of the cross-section of the TCF is shown in Fig. 1. The cladding diameter is the standard 125 μm and

Manuscript received September 11, 2013; revised September 24, 2013; accepted October 11, 2013. Date of publication October 17, 2013; date of current version November 6, 2013. This work was supported by the Consejo Nacional de Ciencia y Tecnología under Contracts CB-2010/157866 and CB-2008/101378. The work of J. R. Guzman-Sepulveda was supported by CONACyT through a M.Sc. scholarship. The work of M. Torres-Cisneros was supported by the projects DAIP-UG 43/11, 01/12, and CONCyTEG GTO-2012-C03-195247.

J. R. Guzman-Sepulveda, V. I. Ruiz-Perez, and D. A. May-Arrioja are with the Fiber and Integrated Optics Laboratory, UAM Reynosa-Rodhe, Universidad Autónoma de Tamaulipas, Reynosa 88779, Mexico (e-mail: jrafael_guzmans@yahoo.com.mx; victoryvan1@hotmail.com; darrioja@uat.edu.mx).

M. Torres-Cisneros is with the Nanobiophotonics Group, Electronics Department, Universidad de Guanajuato, Guanajuato 36885, Mexico (e-mail: mtorres@ugto.mx).

J. J. Sanchez-Mondragon is with the Optics Department, Instituto Nacional de Astrofísica, Optica y Electrónica, Puebla 72000, México (e-mail: delta_dirac@hotmail.mx).

Color versions of one or more of the figures in this letter are available online at http://ieeexplore.ieee.org.

Digital Object Identifier 10.1109/LPT.2013.2286132

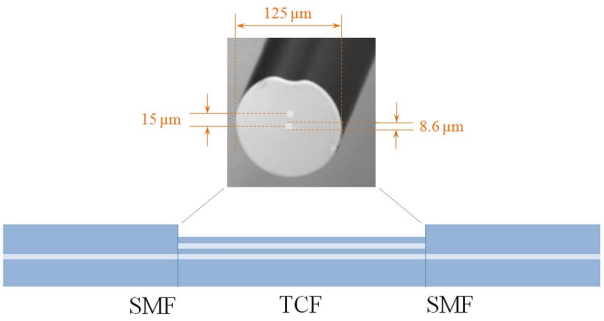

Fig. 1. Schematic of the TCF salinity sensor.

it has two cores, both with diameter of 8.6 μm. One of the cores is located at the center of the fiber while the other is located at a center-to-center separation distance of 15 μm from the central core. According to the fiber manufacturer (ACREO Fiberlab, in Sweden), the RI of the cores and the cladding are 1.448 and 1.443, respectively, which lead to a numerical aperture N.A. $\approx$ 0.12. Since one of the cores of the TCF is located at the center of the fiber, the TCF can be spliced directly to standard single mode fibers (SMF) without the need of special or complex procedures. Furthermore, the characteristics of the fiber, namely separation between the cores and the refractive indices of the cores and the cladding, allow overlapping between the modes in the cores thus leading the TCF to operate basically as an in-fiber directional coupler.

The sensor is fabricated by splicing a section of TCF between two SMFs, as shown in Fig. 1, which leads to the following practical assumptions: only the central core is excited at the beginning of the section of TCF by the input SMF and, since the TCF response will be collected through the central core by the output SMF, the central core is treated as the transmitting core while the external core is treated as the coupling core. Under such assumption, the principle of operation of the sensor is basically a directional coupler with only one core excited. Therefore, the electric field in the transmitting core, as a function of the propagation distance z, can be calculated, in general as [13],

$$A = \cos\left(\sqrt{\kappa^2+\delta^2}\,z\right) + j\frac{\delta}{\sqrt{\kappa^2+\delta^2}}\sin\left(\sqrt{\kappa^2+\delta^2}\,z\right), \quad (1)$$

where $\delta = \Delta\beta/2$ (i.e. $\Delta\beta$ is the difference between the propagation constants of the individual cores), and κ is the coupling coefficient between the cores. When both cores have the same propagation constant (i.e. same RI of core and cladding), then $\Delta\beta = 0$ and Eq. (1) leads to the well known $\cos^2(\kappa z)$ solution for the normalized intensity in the transmitting core of the directional coupler. Initially, this is the case for the TCF if it has not suffered any modification.

In order for the TCF to be sensitive to the surrounding media, the cladding around the off-axis core is controllably removed by means of wet chemical etching. By removing the cladding only around the off-axis core, the central core will remain unaltered at all times. Therefore, any changes in the TCF response will be only due to the interaction between the off-axis core and the surrounding environment. The interaction with the surrounding media will induce changes on the effective RI of the off-axis core and this, in turn, will manifest not only in variations on the coupling coefficient but also in a difference between the propagation constants so the general solution shown in Eq. (1) cannot be longer reduced to a simpler form.

In order to sketch the behavior of the spectral response of the TCF after being etched, Eq. (1) can be evaluated for all the wavelengths within the spectral window of interest assuming a fixed length of the coupler ($z = L_{TCF}$) and introducing the corresponding difference between the propagation constants of the cores. After developing the analytical approach, the TCF is expected to change in the following way as it is surrounded by media with different RI: red shift of the spectral response is expected as the external RI increases and, due to the difference between the propagation constants, the contrast of the spectral response is also enhanced at the same time. From the point of view of the directional coupler, the contrast enhancement as the external RI increases is related to the fact that a more symmetric structure is being formed as the RI of the external media approaches the RI of the fiber cladding. Therefore, since the degree of salinity of water is correlated with different RI of the solution, the coupler-like behavior of the TCF can be manipulated in order to achieve a salinity sensor based on the spectral shifts due to the interaction between the off-axis core of the TCF and the external surrounding media.

III. Experimental Measurements

The experimental setup for testing the salinity sensor based on TCF consists of a broadband light source (i.e. super luminescent diode, SLD, centered at 1580 nm), a 5 cm-long section of TCF spliced between two SMFs, and an optical spectrum analyzer (OSA). In order to remove the cladding material only around the off-axis core, to eliminate the surface tension effects, and to provide mechanical support to the fiber after being etched, the TCF was fixed to the bottom of a channel and carefully aligned to have the external core facing up, along the entire interaction length (i.e. total length of the TCF). The TCF cladding was etched using a solution of Hydrofluoric Acid known as Buffered Oxide Etchant (BOE), which slowly removes the cladding material thus allowing detecting the starting point of the interaction between the external core and the surrounding liquid, i.e. when the spectral response starts to shift. In fact, by controlling the etching time the sensitivity of the sensor can be effectively controlled due to the strength of the interaction of the TCF and the surrounding media directly depends on the thickness of the cladding around the off-axis core.

The sensor was tested for salinity measurement by preparing several Sodium Chloride (NaCl) aqueous solutions. Based on the NaCl concentration, the aqueous solutions were classified into two sets: the high-concentration solutions, ranging from 0 to 5 M, and the low-concentration solutions, ranging from 0 to 1 M. The RI of the solutions exhibit linear dependency with respect to the concentration of the solution for both tested ranges and represent changes in the RI of the solution from 1.3160 to 1.3603 and from 1.3160 to 1.3262, respectively,

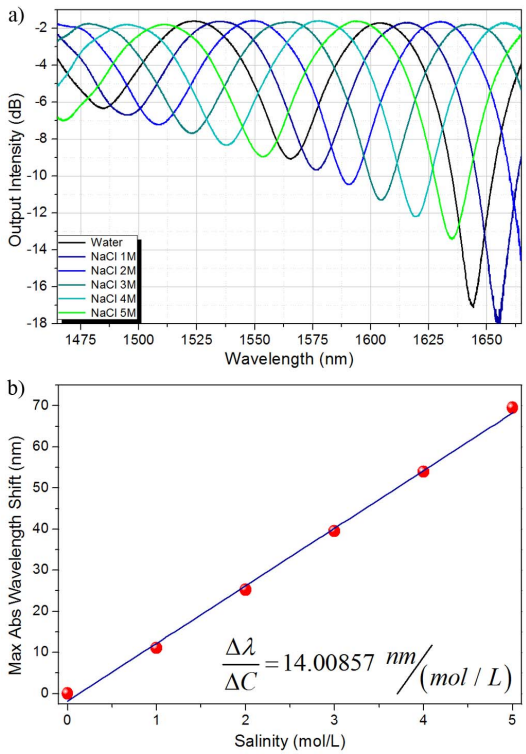

Fig. 2. a) Spectral response of the TCF salinity sensor. b) Wavelength shift for the NaCl concentration range from 0 to 5 M.

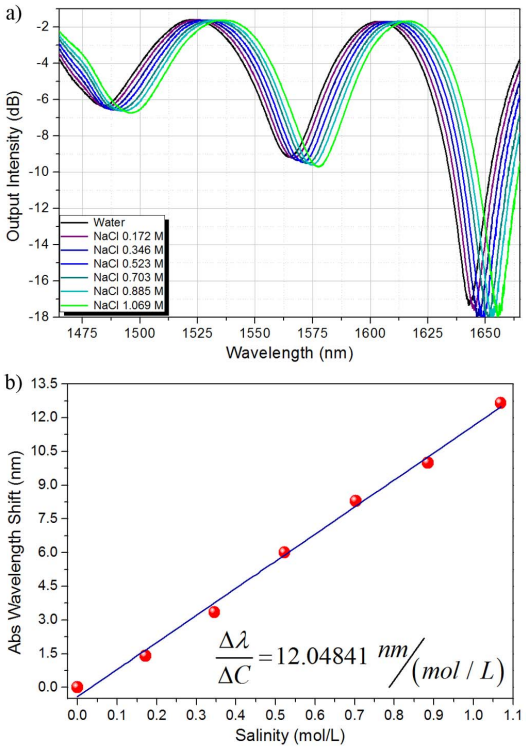

Fig. 3. a) Spectral response of the TCF salinity sensor. b) Wavelength shift for the NaCl concentration range from 0 to 1 M.

at room temperature (20 °C) and operation wavelength of 1550 nm [14]. As mentioned before, the interaction between the TCF and the surrounding liquid is achieved by exposing the outer core through chemical etching. In this case, the etching time was 299 min, and assuming a constant etching rate of 130 nm/min should result in a cladding thickness of the outer core of 4.5 μm approximately. Fig. 2(a) shows the spectral response of the salinity sensor for the solutions set ranging from 0 to 5 M. It can be observed that, in the case of the high-concentration range, a total wavelength shift of 69.50 nm was obtained. When the wavelength shift of the central valley is plotted as a function of the NaCl concentration, as shown in Fig. 2(b), a highly linear response is obtained indicating a sensitivity of 14.0085 nm/M, with $R^2 = 0.99713$, which confirms the reliability of the obtained result.

Once the sensor response was evaluated in the high-concentration range, the sensor was then tested for low-concentration solutions. Evaluating the sensor response in the low-concentration range not only demonstrates the capability to perform salinity measurements for smaller concentrations with high sensitivity but also allows sketching the limit resolution of the sensor. Fig. 3(a) shows the spectral response of the TCF salinity sensor for the concentration range from 0 to 1.069 M. Despite the fact that the wavelength shift is reduced due to the smaller RI variation, the sensor response for each solution can be still clearly identified and a total wavelength shift of 12.65 nm was obtained.

The wavelength shift as a function of salinity is also shown in Fig. 3(b). As expected, the response remains highly linear with an $R^2 = 0.99473$ and a sensitivity of 12.0484 nm/M. It can be noticed that the sensitivity slightly decreases as compared to the case of high-concentration range. This could be related to slight variations of the salinity values during the preparation of the saline solutions. Considering that the spectrum was acquired using an Anritsu MS9740A OSA with a resolution of 0.1 nm and an accuracy of $\pm$ 2 pm, the estimated resolution for the high- and low-concentration regime are 7.1942×10^{-3} M and 8.4506×10^{-3} M, respectively. We should also mention that the solubility of NaCl in water is nearly temperature independent, increasing almost linearly from 357 g/L of water at 0 °C to 400 g/L of water at 100 °C [15], which is equivalent to concentrations ranging from 6.1431 to 6.8446 M. Therefore, we do not observe any alteration of the sensor response after prolonged soaking in the saline solution after several hours due to settling of the NaCl. Additionally flushing the sensor with clean water is not strictly required between measurements, as long as the new concentration flows a sufficient time to entirely remove the previous saline solution. However, flushing is recommended if the sensor will not be used after removing the saline solution in order to avoid any residue on the TCF surface.

Considering that the sensor operates based on the spectral shift of the TCF response, temperature effects need to be taken into account. In fact, since the RI of the saline solutions is also temperature-dependent we need to decouple the thermo-optic effects from the TCF fiber. This is achieved by first taking the temperature dependence of the TCF, before the etching process, in the temperature range from 23 °C to 100 °C. The spectral shift of the TCF response as a function of temperature is shown in Fig. 4 (black curve). A total red shift of approximately 3.3 nm was obtained for this temperature increment of 77 °C. The linear fit of the experimental

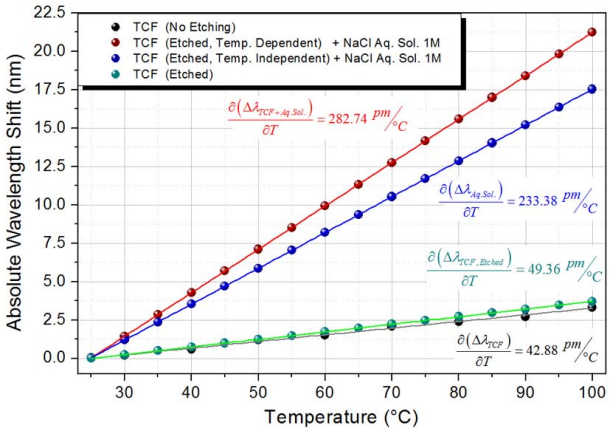

Fig. 4. Temperature dependence of the TCF-based salinity sensor for constant concentration equals to 1 M.

measurements suggest a monotonic temperature dependence of 42.88 ± 1.18 pm/°C, which is in good agreement with the sensitivity reported for a high-temperature sensor based on the same TCF [16]. Numerical fitting to the experimental results, using COMSOL Multiphysics® to obtain κ and MATLAB® to evaluate Eq. (1), provide a thermo-optic coefficient (TOC) for the TCF of 6.35×10^{-5} °C^{-1}. Numerical fitting was also used for the low-concentration range results from Fig. 3 in order to obtain the remaining cladding on top of the off-axis core, which suggests a thickness of 2.77 μm (after 299 min of etching).

After determining the actual fiber diameter and the TOC of the TCF, numerical simulations were performed to disclose the temperature dependence of the sensor for the particular concentration of 1M. The TOC of the saline solution is assumed to be -1.2×10^{-4} °C^{-1} [17], which is similar to the TOC of water. As shown in Fig. 4 (red curve), the spectral response of the sensor is estimated to shift 21.24 nm for the temperature range from 25 °C to 100 °C when the contributions of the TCF and the saline solution are both considered. On the other hand, as shown in Fig. 4 (blue curve), the sensor is estimated to shift 17.53 nm for the temperature range from 25 °C to 100 °C when only the contribution of the saline solution is considered. Since both responses are highly linear, the contribution of the etched TCF can be estimated by subtracting the curve where only the liquid contribution is considered from the curve where both contributions are considered, as shown in Fig. 4 (green curve). A total shift of 3.71 nm is obtained for the temperature range from 25 °C to 100 °C. The spectral shift due to the contribution of the etched TCF is slightly larger than that obtained for the TCF before the etching. Although the temperature contribution of the TCF is small, temperature compensation will be required to guarantee accurate measurements.

We should also notice that in the case of the high-concentration measurements, see Fig. 2, the wavelength shift almost cover the whole free spectral range (FSR) for the maximum salinity value. Nevertheless, the FSR can be easily controlled by changing the length of the TCF, the FSR increases as the length of the section of TCF is reduced. As mentioned before, the sensitivity of the sensor can be also modified by controlling the thickness of cladding of the external core and the surrounding medium. The present sensor corresponds to the case of maximum sensitivity. It is worth to highlight that the sensor sensitivity is at least 19 better as compared to the highest salinity sensor reported to the best of our knowledge [7].

IV. Conclusion

In summary, a novel, simple, cost-effective, and high sensitive salinity sensor based on a TCF has been demonstrated. Sensitivities of 14.00857 nm/(mol/L) and 12.04841 nm/(mol/L) were achieved for the NaCl concentration ranges from 0 to 5 M and from 0 to 1 M, respectively. The achieved sensitivity is approximately 19 times larger than that recently reported for polymide-coated photonic crystal fibers.

References

[1] D. J. Gentleman and K. S. Booksh, "Determining salinity using a multi-mode fiber optic surface plasmon resonance dip-probe," *Talanta*, vol. 68, no. 3, pp. 504–515, 2006.

[2] O. López, D. Gomis, and A. Sánchez-Arcilla, "Hydrographic and hydrodynamic characteristics of the eastern basin of the Bransfield Strait (Antarctica)," *Deep Sea Res. I, Oceanograph. Res. Papers*, vol. 46, no. 10, pp. 1755–1778, 1999.

[3] R. C. Millard and G. Seaver, "An index of refraction algorithm for seawater over temperature, pressure, salinity, density, and wavelength," *Deep Sea Res. A, Oceanograph. Res. Papers*, vol. 37, no. 12, pp. 1909–1926, 1990.

[4] L. Men, P. Lu, and Q. Chen, "A multiplexed fiber Bragg grating sensor for simultaneous salinity and temperature measurement," *J. Appl. Phys.*, vol. 103, no. 5, pp. 053107-1–053107-7, 2008.

[5] L. Marrec, *et al.*, "In-situ optical fibre sensors for temperature and salinity monitoring," in *Proc. IEEE Eur. Oceans*, Jun. 2005, pp. 1276–1278.

[6] J. Cong, X. Zhang, K. Chen, and J. Xu, "Fiber optic Bragg grating sensor based on hydrogels for measuring salinity," *Sens. Actuators B, Chem.*, vol. 87, no. 3, pp. 487–490, 2002.

[7] C. Wu, B. O. Guan, C. Lu, and H. Y. Tam, "Salinity sensor based on polyimide-coated photonic crystal fiber," *Opt. Express*, vol. 19, no. 21, pp. 20003–20008, 2011.

[8] H. A. Rahman, S. W. Harun, M. Yasin, and H. Ahmad, "Fiber optic salinity sensor using fiber optic displacement measurement with flat and concave mirror," *IEEE J. Sel. Topics Quantum Electron.*, vol. 18, no. 5, pp. 1529–1533, Sep./Oct. 2011.

[9] Y. Zhao, X. Zhang, T. Zhao, B. Yuan, and S. Zhang, "Optical salinity sensor system based on fiber-optic array," *IEEE Sensors J.*, vol. 9, no. 9, pp. 1148–1153, Sep. 2009.

[10] L. V. Nguyen, M. Vasiliev, and K. Alameh, "Three-wave fiber Fabry–Pérot interferometer for simultaneous measurement of temperature and water salinity of seawater," *IEEE Photon. Technol. Lett.*, vol. 23, no. 7, pp. 450–452, Apr. 1, 2011.

[11] S. Wang, J. Wang, G. Li, and L. Tong, "Modeling optical microfiber loops for seawater sensing," *Appl. Opt.*, vol. 51, no. 15, pp. 3017–3023, 2012.

[12] S. Robinson and R. Nakkeeran, "Photonic crystal based sensor for sensing the salinity of seawater," in *Proc. IEEE ICAESM*, Mar. 2012, pp. 495–499.

[13] Y. Murakami and S. Sudo, "Coupling characteristics measurements between curved waveguides using a two-core fiber coupler," *Appl. Opt.*, vol. 20, no. 3, pp. 417–422, 1981.

[14] D. R. Lide, "Concentrative properties of aqueous solutions: Density, refractive index, freezing point depression, and viscosity," in *CRC Handbook of Chemistry and Physics*, 90th ed. Boca Raton, FL, USA: CRC Press, 2010.

[15] J. Burgess, *Metal Ions in Solution* (Ellis Horwood Series in Chemical Science). Hoboken, NJ, USA: Wiley, 1979.

[16] P. Rugeland and W. Margulis, "Revisiting twin-core fiber sensors for high-temperature measurements," *Appl. Opt.*, vol. 51, no. 25, pp. 6227–6232, 2012.

[17] Y. Zhao and Y. Liao, "Novel optical fiber sensor for simultaneous measurement of temperature and salinity," *Sens. Actuators B, Chem.*, vol. 86, no. 1, pp. 63–67, 2002.